Unconventional Polarization-Switching Mechanism in $(\mathrm{Hf}, \mathrm{Zr})\mathrm{O}_2$ Ferroelectrics and Its Implications

Yao Wu[1,*] Yuke Zhang,[1,*] Jie Jiang,[1] Limei Jiang,[1] Minghua Tang,[1] Yichun Zhou,[1] Min Liao,[1,†] Qiong Yang[1,‡] and Evgeny Y. Tsymbal[2,§]

[1]*Hunan Provincial Key Laboratory of Thin Film Materials and Devices, School of Materials Science and Engineering, Xiangtan University, Xiangtan, Hunan 411105, China*
[2]*Department of Physics and Astronomy & Nebraska Center for Materials and Nanoscience, University of Nebraska, Lincoln, Nebraska 68588, USA*

HfO$_2$-based ferroelectric thin films are promising for their application in ferroelectric devices. Predicting the ultimate magnitude of polarization and understanding its switching mechanism are critical to realize the optimal performance of these devices. Here, a generalized solid-state variable cell nudged elastic band method is employed to predict the switching pathway associated with domain-wall motion in (Hf, Zr)O$_2$ ferroelectrics. It is found that the polarization reversal pathway, where threefold coordinated O atoms pass across the nominal unit-cell boundaries defined by the Hf/Zr atomic planes, is energetically more favorable than the conventional pathway where the O atoms do not pass through these planes. This finding implies that the polarization orientation in the orthorhombic $Pca2_1$ phase of HfO$_2$ and its derivatives is opposite to that normally assumed, predicts the spontaneous polarization magnitude of about 70 μC/cm^2 that is nearly 50% larger than the commonly accepted value, signifies a positive intrinsic longitudinal piezoelectric coefficient, and suggests growth of ferroelectric domains, in response to an applied electric field, structurally reversed to those usually anticipated. These results provide important insights into the understanding of ferroelectricity in HfO$_2$-based ferroelectrics.

The modern theory of polarization predicts that the electric polarization **P** is a multivalued quantity which is only well defined modulo "polarization quantum" $2e\mathbf{R}/\Omega$, where **R** is a lattice vector, Ω is the primitive-cell volume, and a factor of 2 stays for spin degeneracy [1–4]. Qualitatively, the multivalued polarization is a consequence of periodicity in a bulk crystal, where shifting an electron from all lattice sites by lattice vector **R** does not change the crystal structure but alters the dipole moment per unit cell by $2e\mathbf{R}$. This multivalued polarization is believed to be irrelevant to a *change* of polarization—the quantity that can be measured in experiment. Once the initial and final polarization states are well defined, the polarization change is expected to be single valued. Nevertheless, the uncertainty remains with respect to the *direction* of ionic motion between the two oppositely polarized states. For example, in a two-dimensional ionic lattice shown in Fig. 1(a), negatively charged ions are displaced downward from their centrosymmetric positions representing polar state 1. Assuming that the lattice can be switched to a new polar state 2 through centrosymmetric state C [Fig. 1(a)] by moving the anions upward (*not* through the cation planes—N pathway), it seems to be natural to attribute polarization pointing up to the state 1 and polarization pointing down to the state 2, dictated by polar displacement of anions downward or upward from their centrosymmetric

positions, respectively. This picture overturns, however, if we assume that switching occurs through centrosymmetric state C' by moving anions downward (*through* the cation planes—T pathway), as shown in Fig. 1(b), across the nominal unit cell boundary. The final state 2 in Fig. 1(b) is macroscopically identical to that in Fig. 1(a), due to periodicity of the crystal structure. In this case, however, using the centrosymmetric state C' as a reference for polar displacement of anions, it is reasonable to assign polarization pointing down to the state 1 and polarization pointing up to the state 2, which is opposite to that assumed for the N pathway.

This uncertainty in the polarization direction depending on the polarization reversal pathway is accompanied by a difference in the polarization change which is expected to be a measurable quantity. Indeed, the final states 2 in Figs. 1(a) and 1(b) are related by one unit cell translation of the anion sublattice, making these states macroscopically identical but belonging to two separate polarization branches differing by polarization quantum $2ec/\Omega$, where c is the lattice constant in the upright direction of the lattice. As a result, polarization change ΔP_N for the N pathway is related to polarization change ΔP_T for the T pathway as $\Delta P_T = \Delta P_N + 2ec/\Omega$. Thus, depending on the polarization switching pathway, the polarization change
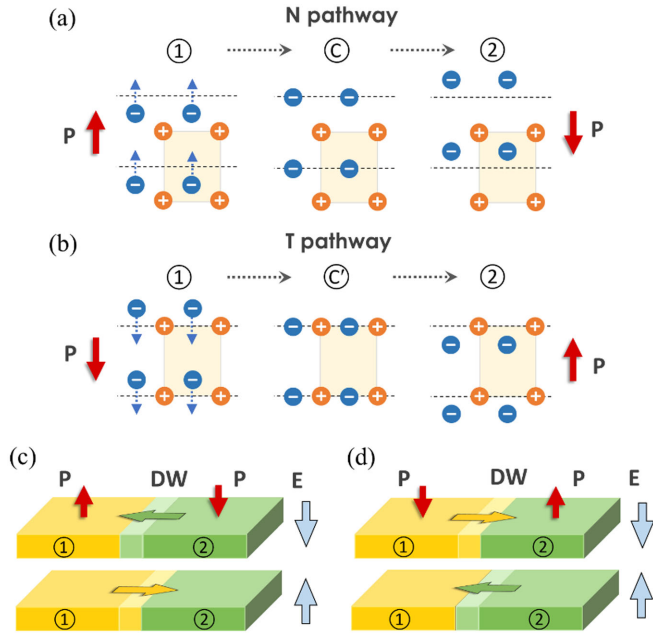
FIG. 1. (a),(b) Polarization reversal in a two-dimensional ionic lattice from state 1 to state 2, where negatively charged ions move upward (N pathway) (a) or downward (T pathway) (b) crossing their centrosymmetric positions (indicated by the dashed lines) in states C and C', respectively. Red arrows and blue dashed arrows indicate polarization orientations and directions of ionic motion, respectively. (c),(d) Polarization switching process in response to applied electric field occurring through domain-wall motion via N (c) and T (d) pathways. Polarization (P) and electric field (E) directions are indicated by red and blue arrows, respectively. Horizontal green and yellow arrows indicate directions of domain-wall motion.

(a measurable quantity) has opposite sign and is different by the polarization quantum.

This observation has implications for the domain-wall motion in response to electric field. For the N pathway of switching in Fig. 1(a), the electric field pointing down pushes negative ions upward resulting in growth of domain 2 in expense of domain 1 [Fig. 1(c), top]. In this case, the domain wall (DW) moves from right to left. If the electric field is reversed, the switching process is also reversed, and the DW moves from left to right [Fig. 1(c), bottom]. This behavior overturns for the T pathway [Fig. 1(b)]. In this case, the electric field pointing down forces domain 1 to grow and domain 2 to shrink, resulting in the DW motion from left to right [Fig. 1(d), top]. For the electric field pointing up, the switching process is reversed and the DW moves from right to left [Fig. 1(d), bottom]. We see therefore that depending on the polarization switching pathway, DW motion occurs in opposite directions.

The polarization dependence on the switching pathway is *not* essential for most ferroelectric materials due to displacement of ions from their centrosymmetric positions being very small compared to the lattice constant. For example, in a perovskite ferroelectric $BaTiO_3$, polar

displacement of Ti atoms is ~ 0.1 Å, while the lattice constant is ~ 4 Å. In this case, polarization reversal occurs through a well-defined centrosymmetric phase (Pm-$3m$ for $BaTiO_3$), while the ionic motion across the unit cell boundaries is energetically prohibitive.

The situation is, however, different for ferroelectric HfO_2. This recently discovered ferroelectric material has advantages of being compatible with the conventional complementary metal-oxide-semiconductor (CMOS) technology, having robust ferroelectricity at the nanometer scale, and thus being promising for device applications [5–13]. Up to date, several crystallographic phases, such as orthorhombic $Pca2_1$ ($Pbc2_1$) [5,14–17] and $Pmn2_1$ [18,19] and rhombohedral $R3m$ [20,21], have been considered to support ferroelectricity in HfO_2. Very recently, Yun *et al.* [22] have unambiguously associated *intrinsic* ferroelectricity in epitaxially grown HfO_2 films with the orthorhombic $Pca2_1$ phase. While there are still debates regarding its stabilization mechanism [23–26], this structural phase is known to represent a lateral array of vertically aligned polar columns of HfO_2 separated by nonpolar columns [Fig. 2(a)]. The vertical displacement of the threefold coordinated oxygen atoms from their centrosymmetric positions in the polar columns is about 0.56 Å. This displacement is comparable to that, 0.71 Å, evaluated with respect to the unit cell boundary, which makes both the N and T switching pathways possible (Fig. 2), resulting in the ambiguity of the polarization direction, as well as its magnitude. Thus, understanding the microscopic mechanism of polarization switching in HfO_2 is not only important *per se*, but also critical for predicting the polarization magnitude that is measured in experiment.
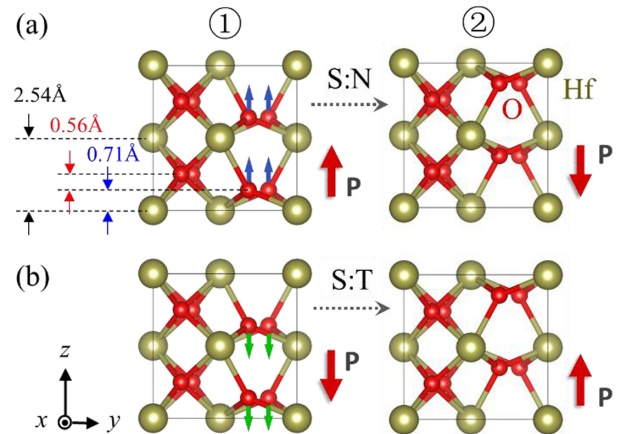

FIG. 2. Atomic structure of HfO_2 and polarization switching pathways between states 1 and 2. S:N (a) and S:T (b) pathways where threefold coordinated O atoms not pass through and passing through the Hf atomic planes, respectively. O atom displacements are indicated by blue and green arrows. Red arrows show pathway-dependent polarization directions for states 1 and 2.

Previous studies have largely focused on the 180° uniform polarization switching in HfO_2-based ferroelectrics where the whole uniformly polarized domain reversed its polarization [18,27–29]. It was argued that possible pathways of polarization switching can be divided into two main categories depending on the motion direction of threefold coordinated O atoms—passing through (T pathway) or not passing through (N pathway) the Hf atomic planes. It was found that the T pathway (going across the orthorhombic $Pbcm$ phase) has a much higher energy barrier than the N pathway (going across the tetragonal $P4_2/nmc$ phase) (Table SII in Supplemental Material [30] summarizes these results). It is known, however, that polarization switching in ferroelectrics is realized via nucleation and growth of ferroelectric domains of reversed polarization, rather than uniform polarization switching [47]. Based on the *most stable* 180° DW structure, the energy barrier for DW motion, where polarization switching occurs via the N pathway, was calculated to be about 1 eV/u.c. [48,49]. (A much lower switching energy barrier was predicted for a topological DW by Choe *et al.* [50], but such a DW has ~1 eV/u.c. higher formation energy.) However, no studies have been performed for polarization switching associated with DW motion via the T pathway.

To address this deficiency, in this Letter, we employ a generalized solid-state variable cell nudged elastic band (VCNEB) method [51] to predict the most energetically favorable switching pathway in ferroelectric HfO_2 and its derivatives. Using this approach, we consistently study polarization reversal pathways in $(Hf, Zr)O_2$ ferroelectrics associated with the DW motion and compare them with other switching mechanisms. We demonstrate that the pathway where O atoms pass through the Hf/Zr atomic planes has the lowest potential barrier thus challenging the previously found results. This finding has significant implications for the understanding of the polarization reversal mechanism in HfO_2-based ferroelectrics, the assignment of polarization orientation to different ferroelectric domains, DW motion under an applied electric field, and the measured magnitude of ferroelectric polarization and piezoelectric response in these materials.

We consider 180° DW motion as the primary mechanism for polarization switching, whereas uniform polarization switching is taken as a reference (see Supplemental Material [30] for computational details). As follows from the previous theoretical studies [48,49] and atomic-scale characterization [52], the most favorable 180° DW structure in HfO_2-based ferroelectrics represents an atomically sharp interface between domains 1 and 2 mimicking the $Pbca$ phase. While uniform polarization reversal may involve displacement of threefold coordinated O atoms either (nearly) *straight* or *crosswise* perpendicular to the DW [30], only the straight O displacement is permitted in the process of 180° DW motion. These pathways of polarization reversal are denoted in Fig. 2 by S:N and S:T are analogous to the N and T pathways in Fig. 1.

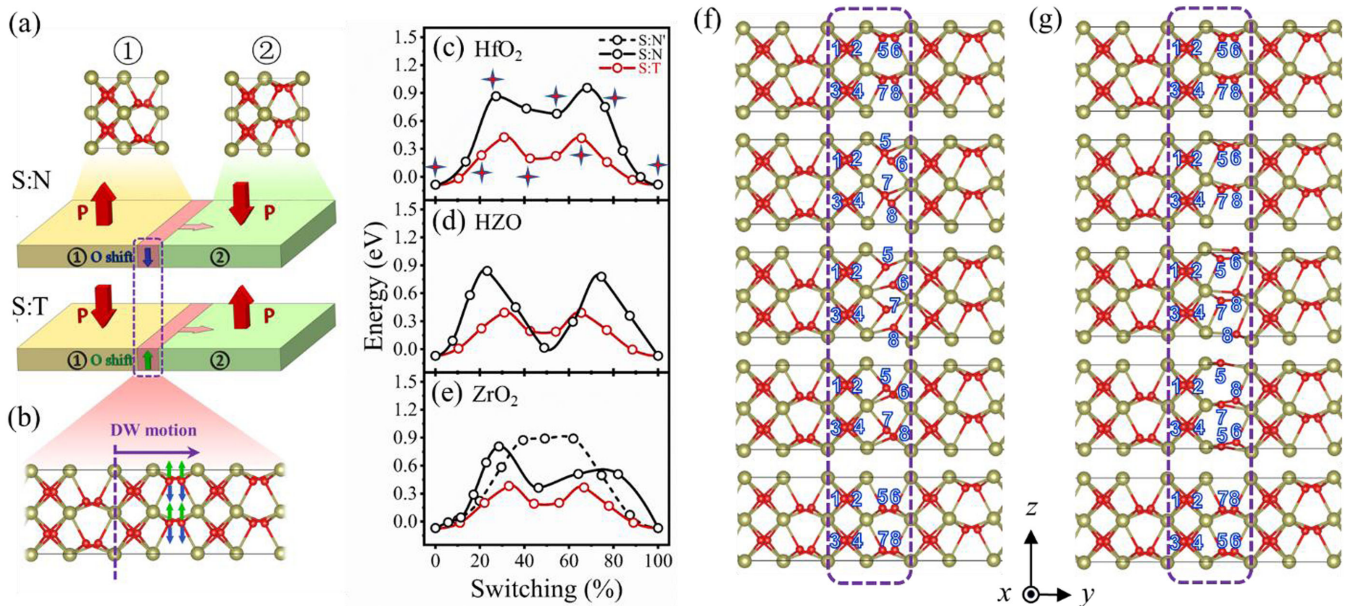Figure 3(a) sketches 180° DW propagation along the S:N and S:T pathways. The DW is set to move rightward, as

FIG. 3. (a) Sketch of 180° DW motion between domains 1 and 2 along the S:N and S:T pathways in $(Hf,Zr)O_2$ ferroelectrics. Red arrows indicate polarization directions of the two ferroelectric domains. (b) DW atomic structure with indicated shifts of threefold coordinated O atoms for the DW motion along S:N (blue arrows) and S:T (green arrows) pathways. (c)–(e) Energy profiles of the whole system for DW motion in HfO_2 (c), HZO (d), and ZrO_2 (e). The total energy of a uniformly polarized domain is set to zero. (f),(g) Atomic evolution of DW motion in HfO_2 along S:N (f) and S:T (g) pathways. Only structural configurations corresponding to the energy points marked by stars in (c) are shown. Dashed rectangles indicate the unit cell where polarization reversal occurs.

shown in Fig. 3(b), driven by displacements of threefold coordinated O atoms along the S:N and S:T pathways [blue and green arrows in Fig. 3(b)] resulting in polarization reversal within the unit cell at the DW. Figures 3(c)–3(e) (black solid lines) show the calculated energy profiles for DW propagation along the S:N pathway in HfO$_2$, HZO, and ZrO$_2$. DW motion exhibits double-barrier energy profiles with the barrier heights of about 1 eV (Table I). Figure 3(f) shows the structural evolution in the process of DW motion for HfO$_2$ (Figs. S9 and S10 [30] for HZO and ZrO$_2$). DW displacement by one unit cell occurs via a successive downward shift of three-fold coordinated O atoms in a unit cell. This leads to an intermediate state, resembling a monoclinic $P2_1/c$ phase (distorted tetragonal $P4_2/nmc$ phase), which is responsible for the local minimum in the energy profiles in Figs. 3(c)–3(e). Because of different local symmetry conditions, the structural evolution along the S:N pathway for the DW motion is different from that obtained for uniform polarization reversal. While, for uniform switching, O atoms shift toward the unit cell center leading to an intermediate state of the tetragonal $P4_2/nmc$ phase of low energy [Fig. S2(a) [30]], for DW motion, this process is prohibited to meet structural continuity with the neighboring cells [Fig. 3(f)] leading to a higher energy barrier (Table I). The simultaneous downward displacement mode of the S:N pathway (named the S:N' pathway and characterized by structural evolution shown in Fig. S11 [30]) is only stable in ZrO$_2$ [black dashed line in Fig. 3(e)].

Polarization switching along the S:T pathway reveals a different behavior. While the calculated energy curves for all three ferroelectrics HfO$_2$, HZO, and ZrO$_2$ also exhibit two peaks along the S:T pathway [Figs. 3(c)–3(e), red solid lines], the associated energy barriers are only about 0.5 eV, nearly half the barriers for the S:N pathway (Table I). As seen from Fig. 3(g) for HfO$_2$ (Figs. S12 and S13 [30] for HZO and ZrO$_2$), upward movement of the O atoms through the Hf atomic planes goes through an $P2_1/c$ intermediate state (distorted $Pbcm$ phase), producing the energy minimum. This structural evolution is qualitatively similar to

that found for the uniform S:T switching of HfO$_2$ [Fig. S2(b) [30], bottom path] and leads to the comparable energy barriers (Table I).

The significantly lower barrier height for the S:T pathway compared to the S:N pathway can be understood from the structural evolution displayed in Fig. S14 [30]. The top (yellow arrows) and bottom (cyan arrows) three-fold coordinated O atoms have opposite displacements along the x direction that are reversed in one domain with respect to the other. When the DW moves along the S:N pathway [Fig. S14(a) [30]], the polar shift of the O atoms along the $-z$ direction is accompanied by their crosswise displacement along the x direction. This leads to structural discontinuity at the DW in the intermediate state and results in a considerable energy cost. On the contrary, when the DW moves along the S:T pathway [Fig. S14(b) [30]], the top threefold coordinated O atoms in one domain continuously transform into the bottom ones in the other domain due to the polar shift of the O atoms along the $+z$ direction with no crosswise displacement in the x direction. This makes the intermediate state for the S:T pathway closer to the ground-state monoclinic $P2_1/c$ phase resulting in the substantially reduced energy barrier.

Importantly, the T pathway appears to be the most favorable not only for the DW motion but also for nucleation of a domain with reversed polarization. We simulate this process by the S:N and S:T polarization reversal within a unit cell of $(Hf, Zr)O_2$ single-domain ferroelectrics [30]. It appears that the S:T pathway exhibits about half the energy barrier of the S:N pathway independent of $(Hf, Zr)O_2$ stoichiometry (Table I). Thus, both domain nucleation and their growth can efficiently occur through the S:T switching mechanism. We note here that the similar energy barriers for unit-cell switching at the DW and within a uniformly polarized domain indicate that the polarization reversal process in HfO$_2$ may be controlled both by domain nucleation and growth and by random unit-cell switching, as has been observed experimentally [53].

Our results challenge the conventional understanding of polarization switching in HfO$_2$-based ferroelectrics and have important implications. First, the S:T switching pathway being responsible for polarization reversal implies that polarization pointing down needs to be assigned to the domain 1 while the polarization pointing up to the domain 2, as shown in Fig. 2(b). This assignment is at odds with the conventional picture where the displacement of the three-fold coordinated O ions from their centrosymmetric positions in the tetragonal $P4_2/nmc$ phase is regarded to be polar leading to the polarization orientations shown in Fig. 2(a). It appears that the orthorhombic $Pbcm$ phase (or its distorted $P2_1/c$ variant) needs to be considered as the centrosymmetric phase reference, leading to polarization orientation shown in Fig. 2(b). The dependence of polarization sign on the switching pathway has been also pointed out recently by Choe *et al.* [50] and Qi *et al.* [54].

TABLE I. Polarization (P), polarization quantum ($2ec/\Omega$), and energy barrier per unit cell (E_b) for uniform polarization (UP) reversal, domain-wall (DW) assisted switching, and unit cell (UC) switching in a single domain for HfO$_2$, HZO, and ZrO$_2$ calculated using the VCNEB method for S:N and S:T pathways.

Crystal	HfO$_2$		HZO		ZrO$_2$	
Pathway	S:N	S:T	S:N	S:T	S:N	S:T
P (μC/cm^2)	51.0	69.7	51.9	67.3	52.3	65.5
$2ec/\Omega$ (μC/cm^2)	120.8		119.2		117.7	
E_b (eV): UP	0.461	0.432	0.349	0.377	0.293	0.362
E_b (eV): DW	1.040	0.509	0.911	0.464	0.876	0.452
E_b (eV): UC	0.918	0.517	0.860	0.480	0.786	0.427

Second, the ultimate polarization magnitude that can be measured in experiment appears to be different from that conventionally assumed. Polarization is calculated using the standard Berry phase method [2] and exhibits several branches separated by the polarization quantum $2ec/\Omega$ (Fig. S24 [30]). The S:N and S:T pathways reveal opposite slopes spanning the total polarization range of $2 \times 2ec/\Omega$. This implies that the polarization change has different signs for the S:N and S:T pathways and their absolute values, P_N and P_T, add up to the value of $2ec/\Omega$ (≈ 120.8 μC/cm^2 for HfO$_2$). Table I shows polarization values calculated for the S:N and S:T pathways, indicating that within the computational accuracy their sum is $2ec/\Omega$ for all three $(\mathrm{Hf}, \mathrm{Zr})\mathrm{O}_2$ stoichiometries considered. Importantly, the predicted P_T value of about 70 μC/cm^2 corresponding to the most energetically favorable switching pathway is larger than the P_N value of about 50 μC/cm^2 that is commonly anticipated for HfO$_2$. This result is plausible for potential application of HfO$_2$-based ferroelectrics where a higher polarization implies a stronger response to external stimulus.

We note that there is a lot of controversy in the literature regarding the experimentally measured values of polarization. This is due to fluctuating quality of films grown in different laboratories, effects of grain boundaries, and defects such as oxygen vacancies [55] which are detrimental to the intrinsic ferroelectricity of HfO$_2$. Recently, however, Yun *et al.* [22] were able to grow Y-doped HfO$_2$ films with a high degree of crystallinity exhibiting a ferroelectric response free from the ambiguities associated with oxygen vacancies and grain boundaries. The measured *intrinsic* polarization was found to be 64 μC/cm^2, i.e., much larger than the nominal 50 μC/cm^2, indirectly signaling the polarization switching mechanism predicted in this work.

The third implication following from our results is the DW motion in response to electric field. Applying an electric field up in Fig. 2 is expected to stimulate growth of domain 2 with polarization parallel to the applied field [Fig. 2(b)], rather than domain 1 [Fig. 2(a)] anticipated in the conventional picture. This prediction can be verified experimentally using the recently developed *in situ* biasing technique in scanning transmission electron microscopy (STEM) [56]. While the precise detection of O atom displacements is challenging, recent advances in STEM make it feasible (e.g., Refs. [15,55]).

The fourth implication is related to the longitudinal piezoelectric coefficient d_{33}. Experimentally, d_{33} varies in magnitude and sign depending on film thickness, deposition method, sample history, *etc.* [57]. Theoretically, for the conventional polarization direction [Fig. 2(a)], d_{33} is predicted to be *negative* [58,59] due to the preserved equilibrium distance of the Hf-O bonds in the switching process. For the opposite polarization associated with the S:T switching pathway [Fig. 2(b)], this mechanism leads to

a *positive* intrinsic longitudinal piezoelectric coefficient. Different sign of the piezoelectric response depending on the polarization switching pathway has been discussed recently by Qi *et al.* [54]. The predicted unconventional switching may also impact pyroelectricity of HfO$_2$ [60].

In summary, we have predicted that ferroelectric polarization switching in $(\mathrm{Hf}, \mathrm{Zr})\mathrm{O}_2$ ferroelectrics associated with domain-wall motion occurs through the S:T pathway, where three-fold coordinated O atoms pass across the nominal unit-cell boundaries defined by the Hf/Zr atomic planes, rather than the conventional S:N pathway. This finding implies that the polarization orientation in the orthorhombic $Pca2_1$ phase of HfO$_2$ and its derivatives is opposite to that normally assumed, predicts the spontaneous polarization magnitude of about 70 μC/cm^2 that is nearly 50% larger than the commonly accepted value, signifies a positive intrinsic longitudinal piezoelectric coefficient, and suggests growth of ferroelectric domains, in response to an applied electric field, structurally reversed to those usually anticipated. Our predictions are important for the understanding of polarization behavior in HfO$_2$-based ferroelectrics, and therefore we hope that they will stimulate efforts to verify them experimentally.

Note added.—Recently, we became aware of the recent study by Silva *et al.* [61] who found a lower energy barrier for the S:T pathway in La-doped HfO$_2$ consistent with our prediction.

[*]These authors contributed equally to this work.
[†]Corresponding author: mliao@xtu.edu.cn
[‡]Corresponding author: qyang@xtu.edu.cn
[§]Corresponding author: tsymbal@unl.edu

[1] R. Resta, Macroscopic electric polarization as a geometric quantum phase, Eur. Phys. Lett. **22**, 133 (1993).
[2] R. D. King-Smith and D. Vanderbilt, Theory of polarization of crystalline solids, Phys. Rev. B **47**, R1651 (1993).
[3] D. Vanderbilt and R. D. King-Smith, Electric polarization as a bulk quantity and its relation to surface charge, Phys. Rev. B **48**, 4442 (1993).

[4] R. Resta and D. Vanderbilt, Theory of polarization: A modern approach, Top. Appl. Phys. **105**, 31 (2007).

[5] T. S. Böscke, J. Müller, D. Bräuhaus, U. Schröder, and U. Böttger, Ferroelectricity in hafnium oxide thin films, Appl. Phys. Lett. **99**, 102903 (2011).

[6] J. Müller, U. Schröder, T. S. Böscke, I. Müller, U. Böttger, L. Wilde, J. Sundqvist, M. Lemberger, P. Kücher, T. Mikolajick, and L. Frey, Ferroelectricity in yttrium-doped hafnium oxide, J. Appl. Phys. **110**, 114113 (2011).

[7] J. Müller, T. S. Böscke, U. Schröder, S. Mueller, D. Bräuhaus, U. Böttger, L. Frey, and T. Mikolajick, Ferroelectricity in simple binary ZrO_2 and HfO_2, Nano Lett. **12**, 4318 (2012).

[8] J. Z. Fan, J. Chen, and J. Wang, Ferroelectric HfO_2-based materials for next-generation ferroelectric memories, J. Adv. Dielectr. **06**, 1630003 (2016).

[9] M. Pešić, F. P. G. Fengler, L. Larcher, A. Padovani, T. Schenk, E. D. Grimley, X. Sang, J. M. LeBeau, S. Slesazeck, U. Schroeder, and T. Mikolajick, Physical mechanisms behind the field-cycling behavior of HfO_2-based ferroelectric capacitors, Adv. Funct. Mater. **26**, 4601 (2016).

[10] X. Tian, S. Shibayama, T. Nishimura, T. Yajima, S. Migita, and A. Toriumi, Evolution of ferroelectric HfO_2 in ultrathin region down to 3 nm, Appl. Phys. Lett. **112**, 102902 (2018).

[11] A. Chouprik, D. Negrov, E. Y. Tsymbal, and A. Zenkevich, Defects in ferroelectric HfO_2, Nanoscale **13**, 11635 (2021).

[12] I. Fina and F. Sánchez, Epitaxial ferroelectric HfO_2 films: Growth, properties, and devices, ACS Appl. Electron. Mater. **3**, 1530 (2021).

[13] U. Schroeder, M. H. Park, T. Mikolajick, and C. S. Hwang, The fundamentals and applications of ferroelectric HfO_2, Nat. Rev. Mater. **7**, 653 (2022).

[14] X. Sang, E. D. Grimley, T. Schenk, U. Schroeder, and J. M. LeBeau, On the structural origins of ferroelectricity in HfO_2 thin films, Appl. Phys. Lett. **106**, 162905 (2015).

[15] T. Shimizu, K. Katayama, T. Kiguchi, A. Akama, T. J. Konno, and H. Funakubo, Growth of epitaxial orthorhombic $YO_{1.5}$-substituted HfO_2 thin film, Appl. Phys. Lett. **107**, 032910 (2015).

[16] T. Li, M. Ye, Z. Sun, N. Zhang, W. Zhang, S. Inguva, C. Xie, L. Chen, Y. Wang, S. Ke, and H. Huang, Origin of ferroelectricity in epitaxial Si-doped HfO_2 films, ACS Appl. Mater. Interfaces **11**, 4139 (2019).

[17] X. Xu, F.-T. Huang, Y. Qi, S. Singh, K. M. Rabe, D. Obeysekera, J. Yang, M.-W. Chu, and S.-W. Cheong, Kinetically stabilized ferroelectricity in bulk single-crystalline HfO_2:Y, Nat. Mater. **20**, 826 (2021).

[18] T. D. Huan, V. Sharma, G. A. Rossetti, and R. Ramprasad, Pathways towards ferroelectricity in hafnia, Phys. Rev. B **90**, 064111 (2014).

[19] T. V. Perevalov, A. K. Gutakovskii, V. N. Kruchinin, V. A. Gritsenko, and I. P. Prosvirin, Atomic and electronic structure of ferroelectric La-doped HfO_2 films, Mater. Res. Exp. **6**, 036403 (2018).

[20] Y. Wei, P. Nukala, M. Salverda, S. Matzen, H. J. Zhao, J. Momand, A. S. Everhardt, G. Agnus, G. R. Blake, P. Lecoeur, B. J. Kooi, J. Íñiguez, B. Dkhil, and B. Noheda, A rhombohedral ferroelectric phase in epitaxially strained $Hf_{0.5}Zr_{0.5}O_2$ thin films, Nat. Mater. **17**, 1095 (2018).

[21] Y. Zhang, Q. Yang, L. Tao, E. Y. Tsymbal, and V. Alexandrov, Effects of strain and film thickness on the stability of the rhombohedral phase of HfO_2, Phys. Rev. Appl. **14**, 014068 (2020).

[22] Y. Yun, P. Buragohain, M. Li, Z. Ahmadi, Y. Zhang, X. Li, H. Wang, J. Li, P. Lu, L. Tao, H. Wang, J. E. Shield, E. Y. Tsymbal, A. Gruverman, and X. Xu, Intrinsic ferroelectricity in Y-doped HfO_2 thin films, Nat. Mater. **21**, 903 (2022).

[23] R. Materlik, C. Künneth, and A. Kersch, The origin of ferroelectricity in $Hf_{1-x}Z_{rx}O_2$: A computational investigation and a surface energy model, J. Appl. Phys. **117**, 134109 (2015).

[24] R. Batra, T. D. Huan, J. L. Jones, G. Rossetti, and R. Ramprasad, Factors favoring ferroelectricity in hafnia: A first-principles computational study, J. Phys. Chem. C **121**, 4139 (2017).

[25] P. Fan, Y. K. Zhang, Q. Yang, J. Jiang, L. M. Jiang, M. Liao, and Y. C. Zhou, Origin of the intrinsic ferroelectricity of HfO_2 from *ab initio* molecular dynamics, J. Phys. Chem. C **123**, 21743 (2019).

[26] S. Kang *et al.*, Highly enhanced ferroelectricity in HfO_2-based ferroelectric thin film by light ion bombardment, Science **376**, 731 (2022).

[27] T. Maeda, B. Magyari-Kope, and Y. Nishi, Identifying ferroelectric switching pathways in HfO_2: First principles calculations under electric fields, in *IEEE International Memory Workshop (IMW)* (IEEE, New York, 2017), p. 7939087.

[28] H. Yang, H.-J. Lee, J. Jo, C. H. Kim, and J. H. Lee, Role of Si doping in reducing coercive fields for ferroelectric switching in HfO_2, Phys. Rev. Appl. **14**, 064012 (2020).

[29] Y.-W. Chen, S.-T. Fan, and C. W. Liu, Energy preference of uniform polarization switching for HfO_2 by first-principle study, J. Phys. D **54**, 085304 (2021).

[30] See Supplemental Material at http://link.aps.org/supplemental/10.1103/PhysRevLett.131.226802 for computational methods, switching pathways for uniform polarization reversal, supplementary structural evolution for DW motion, one unit cell polarization reversal in a single domain, and calculations of spontaneous polarization using the Berry phase method and the Born effective charge method, which includes Refs. [31–46].

[31] G. Kresse and J. Furthmmüller, Efficient iterative schemes for *ab initio* total-energy calculations using a plane-wave basis set, Phys. Rev. B **54**, 11169 (1996).

[32] J. P. Perdew, K. Burke, and M. Ernzerhof, Generalized gradient approximation made simple, Phys. Rev. Lett. **77**, 3865 (1996).

[33] S. Clima, D. Wouters, C. Adelmann, T. Schenk, U. Schroeder, M. Jurczak, and G. Pourtois, Identification of the ferroelectric switching process and dopant-dependent switching properties in orthorhombic HfO_2: A first principles insight, Appl. Phys. Lett. **104**, 092906 (2014).

[34] S. Dutta, H. Aramberri, T. Schenk, and J. Íñiguez, Effect of dopant ordering on the stability of ferroelectric hafnia, Phys. Status Solidi RRL **14**, 2000047 (2020).

[35] G. Henkelman and H. Jónsson, Improved tangent estimate in the nudged elastic band method for finding minimum energy paths and saddle points, J. Chem. Phys. **113**, 9978 (2000).

[36] X. Y. Li, Q. Yang, J. X. Cao, L. Z. Sun, Q. X. Peng, Y. C. Zhou, and R. X. Zhang, Domain wall motion in perovskite ferroelectrics studied by the nudged elastic band method, J. Phys. Chem. C **122**, 3091 (2018).

[37] S. S. Behara and A. Van der Ven, Ferroelectric HfO_2 and the importance of strain, Phys. Rev. Mater. **6**, 054403 (2022).

[38] J.-H. Yuan, G.-Q. Mao, K.-H. Xue, N. Bai, C. Wang, Y. Cheng, H. Lyu, H. Sun, X. Wang, and X. Miao, Ferroelectricity in HfO_2 from a coordination number perspective, Chem. Mater. **35**, 94 (2023).

[39] S.-T. Fan, Y.-W. Chen, and C. W. Liu, Strain effect on the stability in ferroelectric HfO_2 simulated by first-principles calculations, J. Phys. D **53**, 23LT01 (2020).

[40] S.-T. Fan, Y.-W. Chen, P.-S. Chen, and C.W. Liu, *Ab initio* study on tuning the ferroelectricity of orthorhombic HfO2, in *2020 International Symposium on VLSI Technology, Systems and Applications (VLSI-TSA)* (IEEE, New York, 2020), p. 92.

[41] S. V. Barabash, D. Pramanik, Y. Zhai, B. Magyari-Kope, and Y. Nishi, Ferroelectric switching pathways and energetics in $(Hf, Zr)O_2$, ECS Trans. **75**, 107 (2017).

[42] W. Wei, G. Zhao, X. Zhan, W. Zhang, P. Sang, Q. Wang, L. Tai, Q. Luo, Y. Li, C. Li, and J. Chen, Switching pathway-dependent strain-effects on the ferroelectric properties and structural deformations in orthorhombic HfO_2, J. Appl. Phys. **131**, 154101 (2022).

[43] Y. Qi, S. Singh, and K. M. Rabe, Polarization switching mechanism in HfO_2 from first-principles lattice mode analysis, arXiv:2108.12538.

[44] J. Wu, Effects of strain on the electronic, optical, and ferroelectric transition properties of HfO_2: *Ab initio* simulation study, J. Phys. Condens. Matter **33**, 295501 (2021).

[45] S. Clima, S. R. C. McMitchell, K. Florent, L. Nyns, M. Popovici, N. Ronchi, L. D. Piazza, J. V. Houdt, and G. Pourtois, First-principles perspective on poling mechanisms and ferroelectric/antiferroelectric behavior of $Hf_{1-x}Zr_xO_2$ for FEFET applications, in *2018 IEEE International Electron Devices Meeting (IEDM)*, 16.5.1 (IEEE, New York, 2018).

[46] W. Zhong, R. D. King-Smith, and D. Vanderbilt, Giant LO-TO splittings in perovskite ferroelectrics, Phys. Rev. Lett. **72**, 3618 (1994).

[47] Y. H. Shin, I. Grinberg, I. W. Chen, and A. M. Rappe, Nucleation and growth mechanism of ferroelectric domain-wall motion, Nature (London) **449**, 881 (2007).

[48] W. Ding, Y. Zhang, L. Tao, Q. Yang, and Y. Zhou, The atomic-scale domain wall structure and motion in HfO_2-based ferroelectrics: A first-principle study, Acta Mater. **196**, 556 (2020).

[49] H.-J. Lee, M. Lee, K. Lee, J. Jo, H. Yang, Y. Kim, S. C. Chae, U. Waghmare, and J. H. Lee, Scale-free ferroelectricity induced by flat phonon bands in HfO_2, Science **369**, 1343 (2020).

[50] D.-H. Choe, S. Kim, T. Moon, S. Jo, H. Bae, S.-G. Nam, Y. S. Lee, and J. Heo, Unexpectedly low barrier of ferroelectric switching in HfO_2 via topological domain walls, Mater. Today **50**, 8 (2021).

[51] D. Sheppard, P. Xiao, W. Chemelewski, D. D. Johnson, and G. Henkelman, A generalized solid-state nudged elastic band method, J. Chem. Phys. **136**, 074103 (2012).

[52] Y. Cheng, Z. Gao, K. H. Ye, H. W. Park, Y. Zheng, Y. Zheng, J. Gao, M. H. Park, J.-H. Choi, K.-H. Xue, C. S. Hwang, and H. Lyu, Reversible transition between the polar and antipolar phases and its implications for wake-up and fatigue in HfO_2-based ferroelectric thin film, Nat. Commun. **13**, 645 (2022).

[53] P. Buragohain, A. Erickson, T. Mimura, T. Shimizu, H. Funakubo, and A. Gruverman, Effect of film microstructure on domain nucleation and intrinsic switching in ferroelectric $Y:HfO_2$ thin film capacitors, Adv. Funct. Mater. **32**, 2108876 (2022); A. Gruverman (private communication).

[54] Y. Qi, S. E. Reyes-Lillo, and K. M. Rabe, "Double-path" ferroelectrics and the sign of the piezoelectric response, arXiv:2204.06999.

[55] P. Nukala, M. Ahmadi, Y. F. Wei, S. de Graaf, E. Stylianidis, T. Chakrabortty, S. Matzen, H. W. Zandbergen, A. Bjorling, D. Mannix, D. Carbone, B. Kooi, and B. Noheda, Reversible oxygen migration and phase transitions in hafnia-based ferroelectric devices, Science **372**, 630 (2021).

[56] Z. Liu, H. Wang, M. Li, L. Tao, T. R. Paudel, H. Yu, Y. Wang, S. Hong, M. Zhang, Z. Ren, Y. Xie, E. Y. Tsymbal, J. Chen, Z. Zhang, and H. Tian, In-plane charged domain walls with memristive behaviour in a ferroelectric flim, Nature (London) **613**, 656 (2023).

[57] P. Buragohain, H. Lu, C. Richter, T. Schenk, P. Kariuki, S. Glinsek, H. Funakubo, J. Íñiguez, E. Defay, U. Schroeder, and A. Gruverman, Quantification of the electromechanical measurements by piezoresponse force microscopy, Adv. Mater. **24**, 2206237 (2022).

[58] J. Liu, S. Liu, J.-Y. Yang, and L. Liu, Electric auxetic effect in piezoelectrics, Phys. Rev. Lett. **125**, 197601 (2020).

[59] S. Dutta, P. Buragohain, S. Glinsek, C. Richter, H. Aramberri, H. Lu, U. Schroeder, E. Defay, A. Gruverman, and J. Íñiguez, Piezoelectricity in hafnia, Nat. Commun. **12**, 7301 (2021).

[60] J. Liu, S. Liu, L. H. Liu, B. Hanrahan, and S. T. Pantelides, Origin of pyroelectricity in ferroelectric HfO_2, Phys. Rev. Appl. **12**, 034032 (2019).

[61] A. Silva, I. Fina, F. Sánchez, J. P. B. Silva, L. Marques, and V. Lenzi, Unraveling the ferroelectric switching mechanisms in ferroelectric pure and La doped HfO_2 epitaxial thin films, Mater. Today Phys. **34**, 101064 (2023).